



Opposite Roles of Wnt7a and Sfrp1 in Modulating Proper Development of Neural Progenitors in the Mouse Cerebral Cortex

Nan Miao^{1†}, Shan Bian^{2†}, Trevor Lee², Taufif Mubarak², Shiyong Huang³, Zhihong Wen⁴, Ghulam Hussain⁵ and Tao Sun^{1,2*}

¹ Center for Precision Medicine, School of Medicine and School of Biomedical Sciences, Huaqiao University, Xiamen, China, ² Department of Cell and Developmental Biology, Weill Cornell Medicine, Cornell University, New York, NY, United States, ³ College of Oceanology and Food Science, Quanzhou Normal University, Quanzhou, China, ⁴ Marine Biomedical Laboratory and Center for Translational Biopharmaceuticals, Department of Marine Biotechnology and Resources, National Sun Yat-sen University, Kaohsiung, Taiwan, ⁵ Department of Physiology, Government College University, Faisalabad, Pakistan

OPEN ACCESS

Edited by:

Susanne Walitza,
Universität Zürich, Switzerland

Reviewed by:

Sudhir Thakurela,
Harvard University, United States
Paola Bovolenta,
Consejo Superior de Investigaciones
Científicas (CSIC), Spain
Claudio Cantù,
Linköping University, Sweden

*Correspondence:

Tao Sun
taosun@hqu.edu.cn

[†]These authors have contributed
equally to this work.

Received: 03 March 2018

Accepted: 28 June 2018

Published: 17 July 2018

Citation:

Miao N, Bian S, Lee T, Mubarak T,
Huang S, Wen Z, Hussain G and
Sun T (2018) Opposite Roles
of Wnt7a and Sfrp1 in Modulating
Proper Development of Neural
Progenitors in the Mouse Cerebral
Cortex. *Front. Mol. Neurosci.* 11:247.
doi: 10.3389/fnmol.2018.00247

The Wingless (Wnt)-mediated signals are involved in many important aspects of development of the mammalian cerebral cortex. How Wnts interact with their modulators in cortical development is still unclear. Here, we show that Wnt7a and secreted frizzled-related protein 1 (Sfrp1), a soluble modulator of Wnts, are co-expressed in mouse embryonic cortical neural progenitors (NPs). Knockout of Wnt7a in mice causes microcephaly due to reduced NP population and neurogenesis, and Sfrp1 has an opposing effect compared to Wnt7a. Similar to Dkk1, Sfrp1 decreases the Wnt1 and Wnt7a activity *in vitro*. Our results suggest that Wnt7a and Sfrp1 play opposite roles to ensure proper NP progeny in the developing cortex.

Keywords: Wnt7a, Sfrp1, cerebral cortex, neural progenitors, antagonist

INTRODUCTION

During development of the mammalian CNS, billions of neurons are produced from proliferating NPs (Rakic, 2009). In the cerebral cortex, NPs are expanded through symmetric and asymmetric division at the VZ and SVZ (Haubensak et al., 2004; Gotz and Huttner, 2005; Homem et al., 2015). The proper control of proliferation, survival and differentiation of NPs is the key step for normal cortical formation (Rakic, 2007, 2009; Zhao et al., 2008; Sun and Hevner, 2014).

A number of signaling pathways that regulate the switch and balance between proliferation and differentiation of NPs have been defined, including the Notch, Sonic hedgehog, fibroblast growth factor, TGF- β /Smads, and Wnt pathways (Chenn and Walsh, 1999; Rowitch et al., 1999; Hirabayashi et al., 2004; Joksimovic et al., 2009; Aguirre et al., 2010; Menendez et al., 2011; Rash et al., 2011). Wnt signaling pathways play crucial roles in neurogenesis (Kuwabara et al., 2009; Durak et al., 2016). For example, the canonical Wnt/ β -catenin pathway is required for NP self-renewal and differentiation (Chenn and Walsh, 2003; Kalani et al., 2008;

Abbreviations: CNS, central nervous system; CP, cortical plate; CRD, cysteine-rich domain; E0.5, embryonic day 0.5; Fz, frizzled; IP, intermediate progenitor; ISH, *in situ* hybridization; IUE, *in utero* electroporation; NP, neural progenitor; P0, postnatal day 0; PFA, paraformaldehyde; qRT-PCR, quantitative real-time PCR; RNAi, RNA interference; RT-PCR, reverse transcription-PCR; Sfrp1, secreted frizzled-related protein 1; shRNA, short hairpin RNA; SVZ, subventricular zone; TGF- β , transforming growth factor- β ; VZ, ventricular zone.

Bengoa-Vergniory et al., 2014; Delaunay et al., 2014; Bengoa-Vergniory and Kypka, 2015; Garriock et al., 2015). Among the Wnt signaling molecules, *Wnt7a* has been shown to be critical in axonal remodeling, guidance, synaptogenesis and neurotransmitter release in the hippocampus (Hall et al., 2000; Cerpa et al., 2008; Ciani et al., 2011, 2015). *Wnt7a* controls neurogenesis through regulating genes involved in both cell cycle control and neuronal differentiation (Qu et al., 2013; Long et al., 2016).

Furthermore, three distinct receptor families have been reported to mediate the Wnt signaling: Fz, RoR, and Ryk (van Amerongen et al., 2008; Angers and Moon, 2009). In the nervous system, Fz regulate a range of functions from neuronal differentiation to cell polarity, axon guidance, and cell survival (Van Raay et al., 2005; Prasad and Clark, 2006; Liu et al., 2008; Kilander et al., 2014; Zhou and Nathans, 2014; Morello et al., 2015; Chailangkarn et al., 2016). Moreover, Sfrps are a family of secreted factors that modulate Wnt-induced β -catenin pathway through selectively sequestering specific Wnts in different neurons by possessing the Wnt-binding frizzled CRD (Dann et al., 2001; Bovolenta et al., 2008; Nathan and Tzahor, 2009; Lavergne et al., 2011). For example, both *Sfrp1* and *Sfrp2* can be the dominant negative inhibitors of *Wnt3a* to inhibit proliferation in the developing chick neural tube (Galli et al., 2006), and *Sfrp2* can negatively regulate the Wnt signaling in the CNS of *Pax6* mutant mice via inhibiting *Wnt7b* (Kim et al., 2001a). *Sfrp1* knockout mice display abnormal cortical morphogenesis (Esteve et al., 2018). However, the precise regulation of Wnts and their antagonist Sfrps in mammalian cortical neurogenesis is still unclear.

In this study, we show that *Wnt7a* and *Sfrp1* are co-expressed in the VZ of mouse embryonic cerebral cortices. Knockout of *Wnt7a* causes microcephaly due to reduced numbers of NPs and decreased neurogenesis. *Sfrp1* showed overexpression leads to a decrease in the NP population. Similar to the known Wnt antagonist *Dkk1*, *Sfrp1* directly blocks the *Wnt1* and *Wnt7a* activity *in vitro*. Our results indicate that opposite effects of *Wnt7a* and *Sfrp1* play an important role in expansion of cortical NPs.

MATERIALS AND METHODS

Animals and Genotyping

The *Wnt7a* knockout mice (*Wnt7a* KO, *Wnt7a*^{-/-}) were generated by mating female *Wnt7a* heterozygous mice (*Wnt7a*^{+/-}) with male *Wnt7a* heterozygous mice (*Wnt7a*^{+/-}). Mice that only have the mutant allele (*Wnt7a*^{-/-}) were *Wnt7a* KO mice, wild-type (WT) mice were used as controls. To achieve knockout of *Wnt7a*, a double-selection gene-replacement construct was designed to insert a neo gene into a NaeI site in the second exon of the *Wnt7a* gene (Parr and McMahon, 1995; Ashrafi et al., 2012).

For staging of embryos, midday of the day of vaginal-plug formation was considered as E0.5; the first 24 h after birth were defined as P0. Animal use was overseen by the Animal Facility at Weill Cornell Medical College (Protocol number

#2011-0062), and was performed according to the institutional ethical guidelines for animal experiments.

Mouse tail-tip biopsies were used for genotyping by PCR reactions using the following primers: for *Wnt7a* KO, forward: 5-CTCTTCGGTGGTAGCTCTGG-3 and reverse-1: 5-TCACGTCCTGCACGACGCGAGCTG-3 (product size: 350 bp); for WT, reverse-2: 5-TCCTTCCCAGACAGTACG-3 (product sizes: 560 bp).

RNA Sequencing (RNA-Seq)

Total RNAs for RNA-seq were extracted from three individual E12.5 mouse cerebral cortices using TRIzol (Invitrogen, United States) according to manufacturer's instructions. The ribosome RNA (rRNA) removal, generation of cDNA library and high-throughput sequencing were performed on the Ion proton platform (Life Technologies, United States) from the NovelBio Bio-Pharm Technology Company (Shanghai, China). Three sets of raw reads were obtained, and data were deposited in Gene Expression Omnibus (GEO¹) under the series number GSE116056. After removing contaminated and low-quality sequences, all reads were mapped onto the Ensembl mouse reference genome. Gene expression level were calculated by RPKM (reads per kilo-bases per million mapped reads).

In Situ Hybridization

In situ hybridization was performed as described: following fixation with 4% PFA, acetylation with acetylation buffer (1.3% triethanolamine, 0.25% acetic anhydride, 20 mM HCl), treatment with proteinase K (5 μ g/ml, IBI Scientific) and pre-hybridization (1 \times SSC, 50% formamide, 0.1 mg/ml Salmon Sperm DNA Solution, 1 \times Denhart, 5 mM EDTA, pH 7.5), brain sections were hybridized with DIG-labeled LNA probes at Tm -22°C overnight. After washing with pre-cooled wash buffer (1 \times SSC, 50% formamide, 0.1% Tween-20) and 1 \times MABT, sections were blocked with blocking buffer (1 \times MABT, 2% blocking solution, 20% heat-inactivated sheep serum) and incubated with anti-DIG antibody (1:1, 500, Roche) at 4°C overnight. Brain sections were washed with 1 \times MABT and Staining buffer (0.1 M NaCl, 50 mM MgCl₂, 0.1 M Tris-HCl, pH 9.5), stained with BM purple (Roche) at room temperature until ideal intensity was reached. The antisense RNA probe (*Sfrp1*, *Wnt7a*, *Wnt7b*, *Pax6*, *Ngn2*, and *Hes5*) was labeled using the DIG RNA labeling Kit (Roche, Switzerland) following the manufacturer's instructions.

Nissl Staining and Measuring Brain Size

Brain sections (14 μ m) were processed through incubation in the subsequent solutions in the following order: ethanol/chloroform (1:1, overnight), 100% ethanol (30 s), 95% ethanol (30 s), distilled water (30 s, twice), cresyl violet (3–5 min), distilled water (2 min, three times), 50% ethanol (2 min), 95% ethanol (5–30 min), 100% ethanol (5 min, twice), xylene (3 min, twice). Thereafter, the sections were mounted with a coverslip.

¹<http://www.ncbi.nlm.nih.gov/geo/>

The *Wnt7a* KO and WT brain images were captured in one picture, and the thickness of the cortex and CP was measured separately. The relative thickness of the cortex and CP in the KO was normalized from dividing the mean length of KO by that of the WT groups. At least three brains, and two chosen areas in each brain section were measured and averaged in each group. All data are presented as mean \pm SEM. *P*-values were calculated using unpaired Student's *t*-test.

RNA and qRT-PCR

The RNAs for RT-PCR from five stages of samples (E12.5, E13.5, E14.5, E15.5, and E17.5), were extracted by TRIzol (Invitrogen, United States), with three mouse cerebral cortices from each age group. Experimental protocols of embryo treatment used here were approved by Weill Cornell Medical College's animal care and use committee. The procedures were carried out in accordance with the approved guidelines. After RNA extraction, the cDNA for RT-PCR was synthesized using high-capacity cDNA Reverse Transcription kit (Applied Biosystems). The qRT-PCR reactions were carried out in the Bio-Rad CFX-384 system, using the reaction mixture SYBR Green Mix (Bio-Rad, United States) with the aforementioned cDNA samples.

β -Actin was used as an internal control, and was used to normalize the relative mRNA expression level. Each group had three biological repetitions, and all experiments were performed in triplicate, and each experiment was repeated at least twice. The qRT-PCR primers are: *Wnt7a*, forward: 5'-CCGAAATGG CCGTTGG-3' and reverse: 5'-CGATGCCGTAGCGGATGT-3' (PCR product: 251 bp); *Sfrp1*, forward: 5'-CAACGTGGGCT ACAAGAAGAT-3' and reverse: 5'-GGCCAGTAGAAGCCGA AG AAC-3' (product size: 249 bp); β -actin, forward: 5'-GGCT GTATTCCCCTCCATCG-3' and reverse: 5'-CCAGTTGGTAA CAATGCCATGT-3' (product size: 245 bp). All data are presented as mean \pm SEM. *P*-values were calculated using unpaired Student's *t*-test.

Tissue Preparation, Immunohistochemistry, and Analysis

Immunohistochemistry was performed as described: mouse brains were fixed in 4% PFA in phosphate-buffered saline (PBS) over night, incubated in 25–30% sucrose in PBS, embedded in OCT and stored at -80°C until use. Brains were sectioned (14–16 μm) using a cryostat. For antigen recovery, sections were incubated in heated (95–100 $^{\circ}\text{C}$) antigen recovery solution (1 mM EDTA, 5 mM Tris, pH 8.0) for 15–20 min, and cooled down for 20–30 min. Before applying antibodies, sections were blocked in 10% normal goat serum (NGS) in PBS with 0.1% Tween-20 (PBT) for 1 h. Sections were incubated with primary antibodies at 4 $^{\circ}\text{C}$ overnight and visualized using goat anti-rabbit IgG–Alexa-Fluor-488 and/or goat anti-mouse IgG–Alexa-Fluor-546 (1:300, Molecular Probes) for 1.5 h at room temperature. Images were captured using a Leica digital camera under a fluorescent microscope (Leica DMI6000B) or a Zeiss confocal microscope.

The following antibodies were used: bromodeoxyuridine (BrdU) (1:50, DSHB), Ki67 (1:500, Abcam), Pax6 (1:30, DSHB),

Tbr1 (1:2500, Abcam), Tbr2 (1:2000, kindly provided by Robert Hevner, University of Washington, Seattle, WA, United States), Ctip2 (1:1000, Abcam), Satb2 (1:1000, Abcam), GFP (1:600, DAKO), Neun (1:300, Chemicon), *Wnt7a* (1:1000, Abcam) and *Sfrp1* (1:1000, Abcam).

Cell counting in the mouse brain sections was performed on a fixed width (200 μm bin) of a representative column in the cortical wall. All sections analyzed were selected from a similar medial point on the anterior-posterior axis. Cell counting was performed in minimal three chosen areas in each brain, and at least three brains were analyzed in each group. Cell counting in each chosen area was repeated at least three times and a mean was obtained. All data are presented as mean \pm SEM. *P*-values were calculated using unpaired Student's *t*-test.

Plasmid DNA Constructs

To clone *Sfrp1*, *Dkk1* and *Wnt7a* coding sequences into *pCAGIG* for IUE, *Sfrp1*, *Dkk1* and *Wnt7a* coding sequences from *pGEM-T* was attached to d2EGFP, a destabilized variant of the wild-type GFP, and then subcloned *d2EGFP-Sfrp1*, *-Dkk1* and *-Wnt7a* coding sequence fragments into *pCAGIG*.

Full length coding sequences (CDSs) for *Sfrp1*, *Dkk1* and *Wnt7a* were cloned using the following primers: *Sfrp1*, forward: 5'-ATTCCGCTCGAGCGGGTCGCCGAGCAACATG GGCGTC-3' and reverse: 5'-ATTCCTAAGGCCTTCCCCAG TCCGCCCCAG-3' (PCR product: 954 bp); *Wnt7a*, forward: 5'-GCACTCGAGCAGCGGGACTATGACCCGAAAGCGC-3' and reverse: 5'-CATTCACCTGACAGTATACATCTCCG TG-3' (PCR product: 1,053 bp); *DKK1*, forward: 5'-CGGAATTC GGAGATGATGGTTGTGTGTGC-3' and reverse: 5'-GGTTT AGTGTCTCTG GCAGGTGTG-3' (PCR product: 826 bp).

The *Sfrp1*, *Dkk1* coding sequences were subcloned into the *pcDNA3.1* vector for the *TOPflash* and *FOPflash luciferase* reporter (Promega, United States) assay.

RNA Interference Design and Efficiency Analysis

To knockdown *Sfrp1*, 4 different *Sfrp1* specific *short hairpin RNA* (*Sfrp1-shRNA*) were designed and cloned into the *pSilencer* vector, separately. To analyze interference efficiency, Neuro2A cells were plated into 6-well plates in triplicate, and were transfected with four *Sfrp1-shRNA* using Lipofectamine 3000 (Invitrogen, United States). Cells were cultured for 2 days and the endogenous *Sfrp1* knockdown efficiency was verified by qRT-PCR. The *shRNA* with the highest knockdown efficiency was selected to perform further IUE in cerebral cortices.

The following oligos were used to clone *Sfrp1-shRNA*: *Sfrp1-shRNA1*, 5'-CACCGCTACAAGAAGATGGTGCTGC TTCAAGAGAGCAGCACCATCTTCTGGTAGCTTTTTTTG-3' (Target site: GCTACAAGAAGATGGTGCTGC, 498–519); *Sfrp1-shRNA2*, 5'-CACCGCCACAACCTTCTCATCATGGTTCAAG AGACCATGATGAGAAAGTTGTGGCTTTTTTTG-3' (Target site: GCCACAACCTTCTCATCATGG, 1,077–1,098); *Sfrp1-shRNA3*, 5'-CACCGCCATTCACAAGTGGGACAAGTTCAAG AGACTTGTCCCCTTGTCCCCTTGTGAATGGCTTTTTTT

G-3' (Target site: GCCACAACCTTCTCATCATGG, 1,130–1,151); *Sfrp1-shRNA4*, 5'-CACCGCAGTTCTTCGGCTTCTACTGTTCAAGAGACAGTAGAAGCCGAAGAAGCTGCTTTTTT G-3' (Target site: GCAGTTCTTCGGCTTCTACTG, 715–736); for negative control, 5'-CACCGTTCTCCGAACGTGTCACGTTCAAGAGAACGTGACACGTTTCGGAGAATTTTTTTG-3'.

In Utero Electroporation

In utero electroporation was performed in E12.5 embryos according to the published protocol (Saito and Nakatsuji, 2001; Saito, 2006; Ito et al., 2014). Briefly, plasmid DNA was prepared using the EndoFree Plasmid Maxi Kit (Qiagen) according to manufacturer's instructions, and diluted to 2 $\mu\text{g}/\mu\text{L}$. DNA solution was injected into the lateral ventricle of the cerebral cortex, and electroporated with five 50-ms pulses at 35V using an ECM830 electro square porator (BTX). Embryos were allowed to develop to E13.5. Animals with their brains electroporated, as detected by the GFP fluorescence under a fluorescent dissection scope (Leica, MZ16F), were selected for further analyses. Cell counting was performed in minimal three chosen areas in each brain, and at least three electroporated brains for each construct were analyzed. Cell counting in each chosen area was repeated at least three times and a mean was obtained.

TOPflash and FOPflash Luciferase Reporter Assay

The coding sequences of the *Wnt7a* and *Wnt1* were amplified by PCR from mouse cDNA. Reporter genes were cloned into *TOPflash* and *FOPflash* vector (Promega, United States). For transfections, mouse Neuro2A cells were suspended in DMEM and plated into 24-well plates in triplicate at 1.5×10^4 cells/100 mL. Adherent cells were co-transfected with 100 ng/mL *luciferase* reporter containing the reporter gene and 60 ng/mL vector (pcDNA3.1 blank vector, pcDNA3.1-*Dkk1* and pcDNA3.1-*Sfrp1*) using Lipofectamine 3000 (Invitrogen, United States). After 48 h, cells were harvested and *luciferase* activity was measured using the *luciferase* reporter assay system (Cat. #E1910, Promega, United States) according to the manufacturer's protocol.

The relative *luciferase* activity was normalized from the mean of pcDNA3.1 blank vector, separately. Each group had three biological repetitions, and experiments were performed in triplicate and each sample was repeated at least three times. All results are presented as mean \pm SEM. *P*-values were calculated using unpaired Student's *t*-test.

Statistical Analysis

All experiments using cultured cells and mouse embryos were repeated at least with three biological replicates. All results are presented as mean \pm standard error of the mean (SEM). *P*-values were determined by unpaired Student's *t*-test for assessing the significance of differences between two treatments (See each figure for details). *P*-values < 0.05 were considered significant. Significant differences were denoted as **P*-values < 0.05 , ***P*-values < 0.01 , ****P*-values < 0.001 .

RESULTS

Wnt7a and Sfrp1 Are Co-expressed in NPs in the VZ

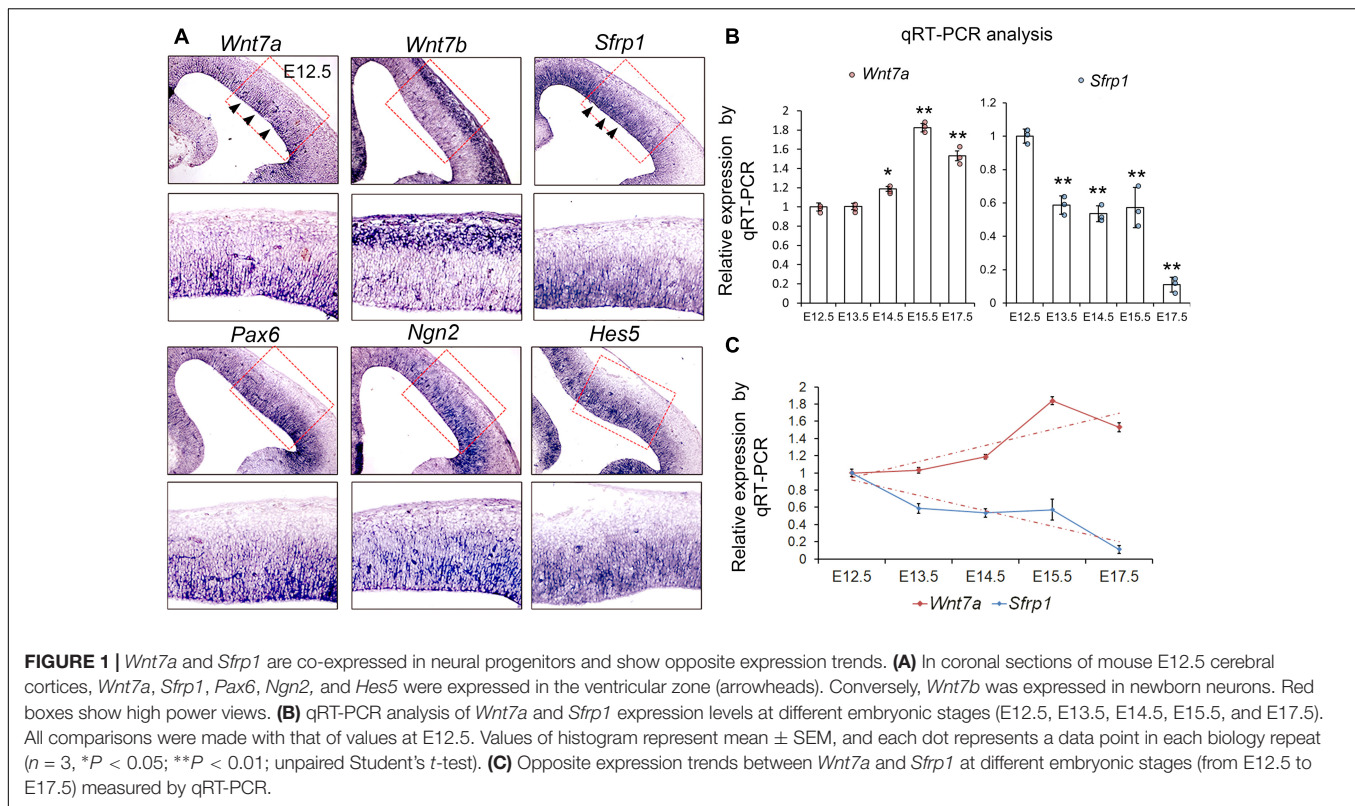
To screen genes that are highly expressed in the mouse E12.5 cerebral cortices, RNA sequencing (RNA-seq) was performed. 30,827,078 and 29,345,746 and 32,038,052 raw sequencing reads, and 28,547,544 and 27,289,172 and 29,753,653 clean reads, respectively, were obtained from three individual E12.5 cortices (Supplementary Table S1). The mapping rates of clean reads are 92.2%, 93.4%, and 92.6% (Supplementary Table S2). Among these genes, *Wnt7a*, *Wnt7b*, and *Sfrp1* showed high expression (RPKM > 500) (Supplementary Figure S1A and Supplementary Table S4). Moreover, *Wnt7b*, *Wnt7a*, and *Wnt5a* displayed higher abundant expression levels than other *Wnt* genes (Supplementary Tables S3, S4).

To verify the RNA-seq data, we examined expression patterns of *Wnt7a*, *Wnt7b*, and *Sfrp1*, and compared them with those of NP markers such as *Pax6*, *Ngn2*, and *Hes5*, and other *Sfrps* such as *Sfrp2*, *Sfrp4*, and *Sfrp5* in the mouse cortex at E12.5 using ISH (Figure 1A and Supplementary Figure S1B). We found that both *Wnt7a* and *Sfrp1* are expressed in the VZ of the E12.5 cortex (Figure 1A). Moreover, expression of *Wnt7a* and *Sfrp1* was co-localized with that of *Pax6*, *Ngn2* and *Hes5*, suggesting that *Wnt7a* and *Sfrp1* are largely expressed in NPs (Figure 1A). Conversely, *Wnt7b* was highly expressed in newborn neurons, and other *Sfrps* such as *Sfrp2* displayed low expression in the cortex (Figure 1A and Supplementary Figure S1B).

Next, we investigated whether expression levels of *Wnt7a* and *Sfrp1* progressively change over embryonic stages at E12.5, E13.5, E14.5, E15.5, and E17.5 using qRT-PCR. *Wnt7a* displayed ascending expression from E12.5 to E15.5 (Figure 1B). *Sfrp1* expression showed a gradual decline from E12.5 to E17.5 (Figure 1C). Compared to *Wnt7a*, *Sfrp1* displays overlapping expression with *Wnt7a* in the VZ and opposite expression levels, implying distinct roles of *Wnt7a* and *Sfrp1* in cortical development.

Wnt7a Positively Regulates Proliferation of NPs and Promotes Neurogenesis

Because of *Wnt7a* expression in the cortical VZ, we investigated whether *Wnt7a* regulates NP proliferation by analyzing cortical development in *Wnt7a* knockout mice (*Wnt7a* KO). The body size of *Wnt7a* KO was indistinguishable from that of WT mice. The cortical size and brain size were measured at P0, P5, and P20 (Figures 2A–C and Supplementary Figure S2). Compared to WT, the cortical size and brain size of *Wnt7a* KO mice were greatly reduced from P0 to P20, suggesting a progressive brain deterioration (Figures 2A–C and Supplementary Figure S2). Moreover, the thickness of the cortical wall was significantly reduced in the brain sections with Nissl staining in *Wnt7a* KO mice (Figures 2B,C). Interestingly, the ratios of cortical size versus brain size were similar between WT and KO, suggesting that the overall brain size is reduced in *Wnt7a* KO mice (Figure 2C and Supplementary Figure S2).



We then examined whether the NP population was changed in E13.5 *Wnt7a* KO mice using immunohistochemistry. NPs can be detected by labeling cells in the G1, S, G2, and M phases using the anti-Ki67 antibody. The number of Ki67⁺ cells was significantly decreased in the E13.5 *Wnt7a* KO cortex, compared to the control (**Figures 2D,E**). The numbers of Sox2⁺ and Pax6⁺ radial glial cells (RGCs), and Tbr2⁺ IPs were also reduced, suggesting an early reduction of NPs (**Figures 2F–K**). Moreover, because Pax6⁺/Tbr2⁺ cells are under transition from RGCs to IPs, we quantified the number of Pax6⁺/Tbr2⁺ cells. While a significant decrease in the number of Pax6⁺/Tbr2⁺ cells was detected in E13.5 *Wnt7a* KO cortex, the percentages of Pax6⁺/Tbr2⁺ cells versus total Pax6⁺ cells and Pax6⁺/Tbr2⁺ cells versus total Tbr2⁺ cells were unchanged, indicating that *Wnt7a* deletion doesn't affect transition of RGCs to IPs (Supplementary Figures S3A–D). In addition, even though the total number of Tbr2⁺ cells was reduced, the percentage of Tbr2⁺ cells versus total DAPI⁺ cells remained the same in WT and *Wnt7a* KO cortices, suggesting that reduction in IPs is in proportion with that of total cells (Supplementary Figures S3E,F).

Next, we examined whether the early loss of NP population is maintained at E15.5. Compared to the controls, the numbers of BrdU⁺, Ki67⁺, Sox2⁺, Tbr1⁺, Pax6⁺, and Tbr2⁺ cells were greatly reduced in E15.5 *Wnt7a* KO cortices, suggesting that the deletion of *Wnt7a* causes a progressive loss of NPs (**Figures 3A–F** and Supplementary Figures S4A,B).

Because the overall organization of cortical layers is becoming clear, and neuronal production is evident at P0, P0 pups were

collected to analyze brain phenotypes without sacrifice of the mother. We examined the expression of Tbr1 (layer VI), Ctip2 (layer V) and Satb2 (layer II, III, and IV) in P0 *Wnt7a* KO and control cortices (Molyneux et al., 2007). The relative positioning of layer markers in the CP was similar to that of the WT, suggesting that overall cortical layer organization is not greatly affected by *Wnt7a* deletion (**Figures 3G,I**). Despite concordance of the position of layer markers, each layer examined was thinner in the *Wnt7a* KO cortex than that in the control, with significantly fewer mature NeuN⁺ neurons found, and great reductions in the number of Tbr1⁺ and Satb2⁺ neurons (**Figures 3G–J**). The Ctip2⁺ neurons showed no appreciable decrease in *Wnt7a* KO mice (**Figures 3I,J**). Moreover, the percentages of Tbr1⁺ and Satb2⁺ cells versus DAPI⁺ cells were unchanged in WT and KO cortices, indicating that the reduction in newborn neurons is in proportion with that of total cells (Supplementary Figure S4C).

Taken together, our results indicate that knockout of *Wnt7a* causes reduced NPs and production of newborn neurons.

Sfrp1 Negatively Regulates Proliferation of NPs

We next examined whether altering *Sfrp1* expression in the cortex has a similar or an opposite effect on NPs as deleting *Wnt7a* expression. The full length cDNA for *Sfrp1* was cloned (*pCAGIG-Sfrp1*) and was ectopically expressed in E12.5 cortices by using IUE, and embryos were analyzed after 24 h. Overexpression of *Sfrp1* resulted in a decreased number of GFP⁺ NPs that are

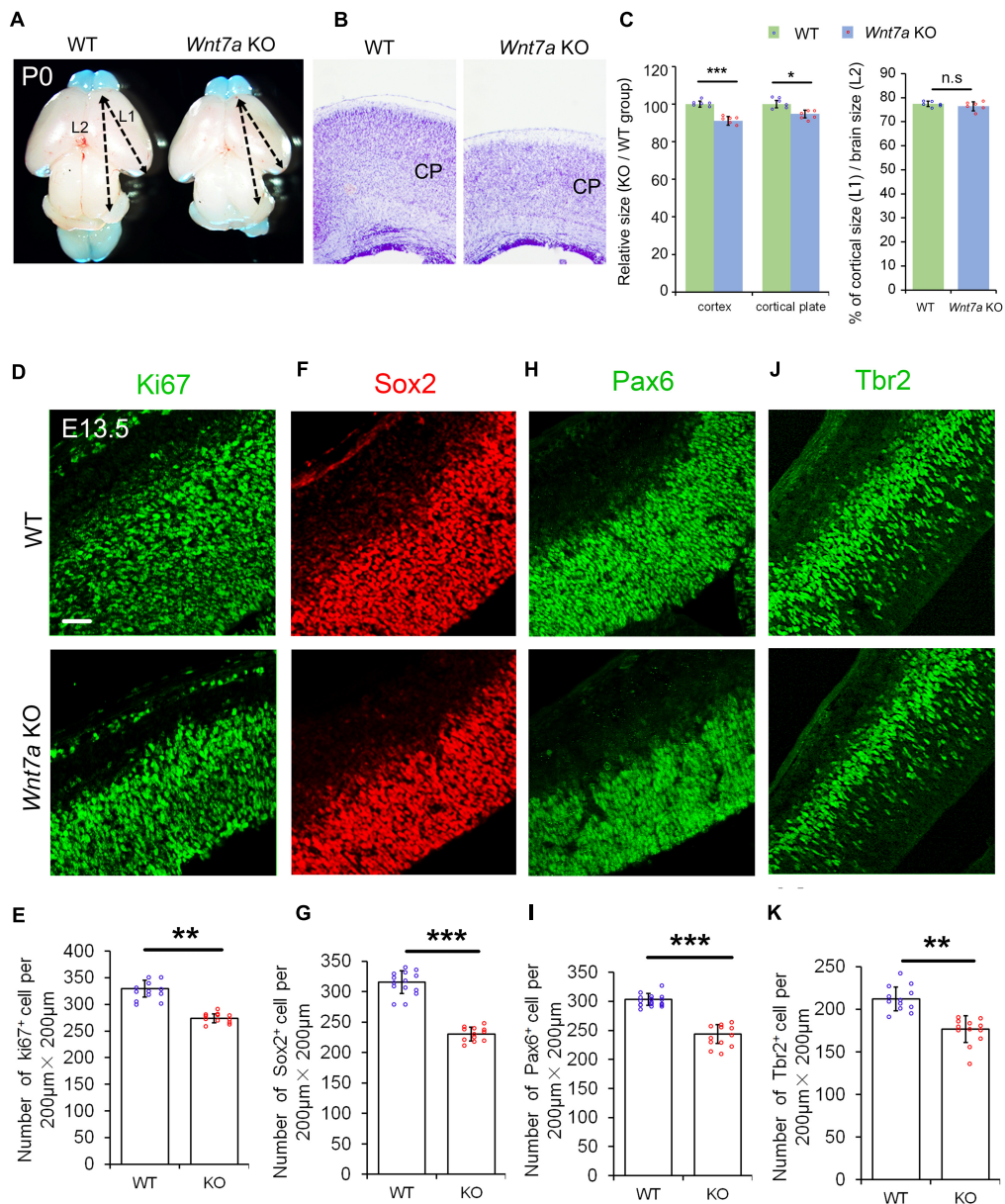
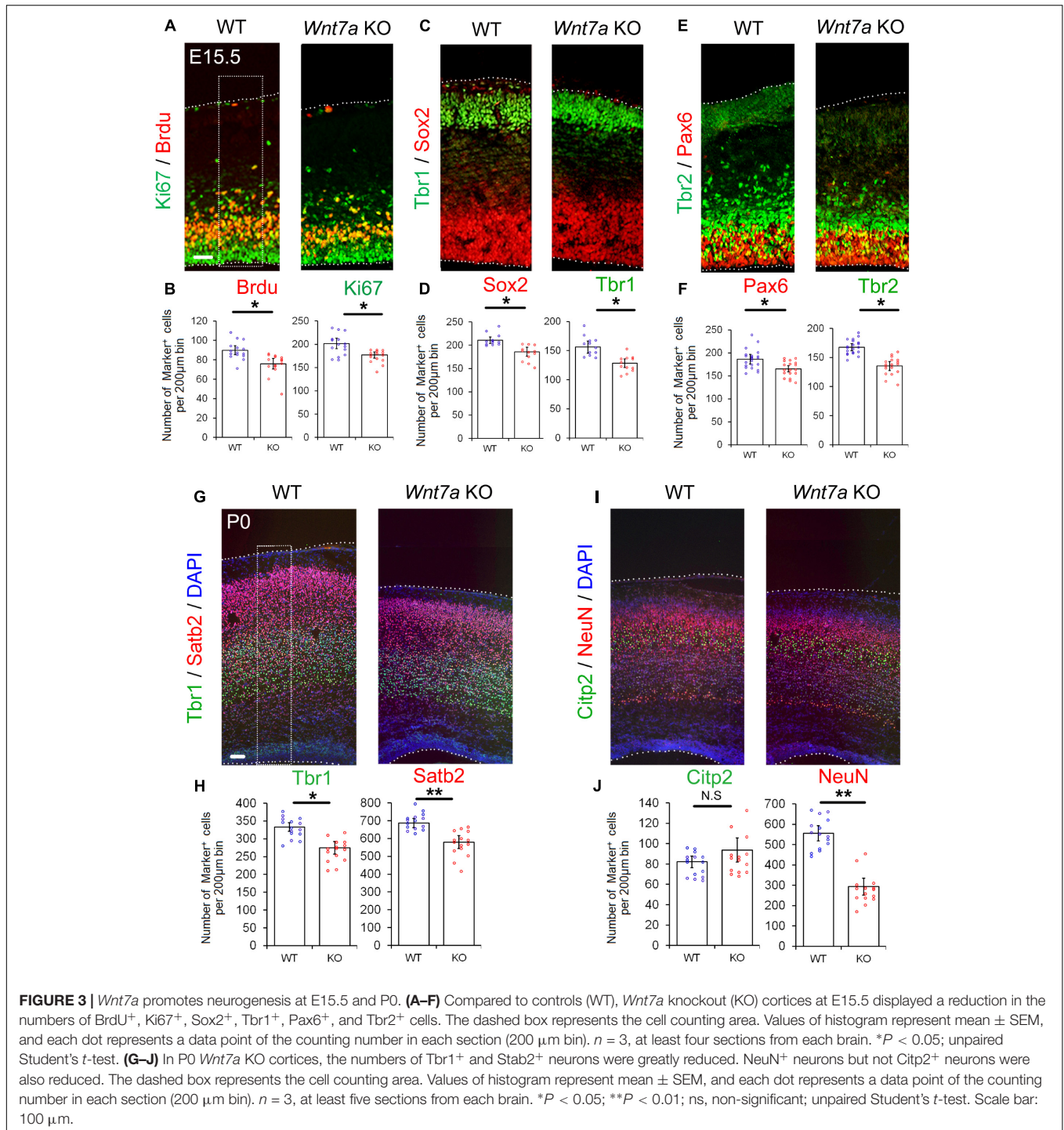


FIGURE 2 | *Wnt7a* positively regulates brain size and proliferation of NPs. **(A)** The cortex of P0 *Wnt7a* knockout (KO) mice was greatly reduced compared to wild type (WT) controls. The arrowheads show the most rostral and caudal regions in the cortex. “L1” represent the cortical length, and “L2” represent the brain length. **(B)** The cortical wall in P0 *Wnt7a* KO mice were thinner than that in WT mice, detected by Nissl staining. CP: cortical plate. **(C)** The relative thickness of the cortex and cortical plate in the KO was normalized from dividing the mean length of *Wnt7a* KO by that of the WT groups. Values of histogram represent mean \pm SEM, and each dot represents a data point of the relative thickness in each section or length in the brain images. $n = 3$ brains, at least two sections from each brain. $*P < 0.05$; $***P < 0.001$; ns, non-significant; unpaired Student’s *t*-test. **(D–K)** The numbers of Pax6⁺ and Tbr2⁺ neural progenitors were greatly reduced in the E13.5 *Wnt7a* KO cortex. Values of histogram represent mean \pm SEM, and each dot represents a data point of the counting number in each section (200 μ m bin). $n = 3$ brains, at least four sections from each brain. $**P < 0.01$; $***P < 0.001$; unpaired Student’s *t*-test. Scale bar: 50 μ m.

double-positive for BrdU⁺, Pax6⁺, Sox2⁺ and Tbr2⁺, compared to those of electroporation of the control (*pCAGIG*) in E13.5 cortices, suggesting a decrease of NPs after *Sfrp1* overexpression (Figure 4).

To test whether the endogenous *Sfrp1* limits the NP numbers *in vivo*, we used *shRNA* designed to outcompete endogenous *Sfrp1* transcripts. The *Sfrp1* knockdown efficiency were verified

in mouse Neuro2A cell by qRT-PCR (Supplementary Figure S5). The construct of *shRNA* (*Sfrp1-sh4*) that shows the highest knockdown efficiency among four tested *shRNAs* was used to perform IUE. Greater proportions of GFP⁺ NPs expressed BrdU, Pax6 and Sox2 were found in the VZ/SVZ following electroporation of the *Sfrp1-sh4* (Supplementary Figures S6A–F). Tbr2⁺ NPs displayed no appreciable increase (Supplementary



Figures S6G,H). These results indicate that *Sfrp1* negatively modulates NP proliferation.

***Sfrp1* Has an Opposite Role of *Wnt7a* in Regulating NP Proliferation**

Based on opposite effect of *Wnt7a* and *Sfrp1* on NP development, we suspected that *Wnt7a* might be regulated by its antagonists

during cortical development. Previous studies have shown that *Dkk1* is an antagonist of *Wnt7a* (Fortress et al., 2013). To examine how the *Wnt7a* antagonist may regulate NP development in the cortex, we over-expressed both *Wnt7a* and *Dkk1* in the VZ of cortex using IUE. While *Wnt7a* promoted expansion of NPs, as shown by an increased number of BrdU⁺ and Pax6⁺ cells, over-expression of *Dkk1* and *Wnt7a* in the VZ dampened *Wnt7a* effects, suggesting an antagonistic regulation of *Dkk1*

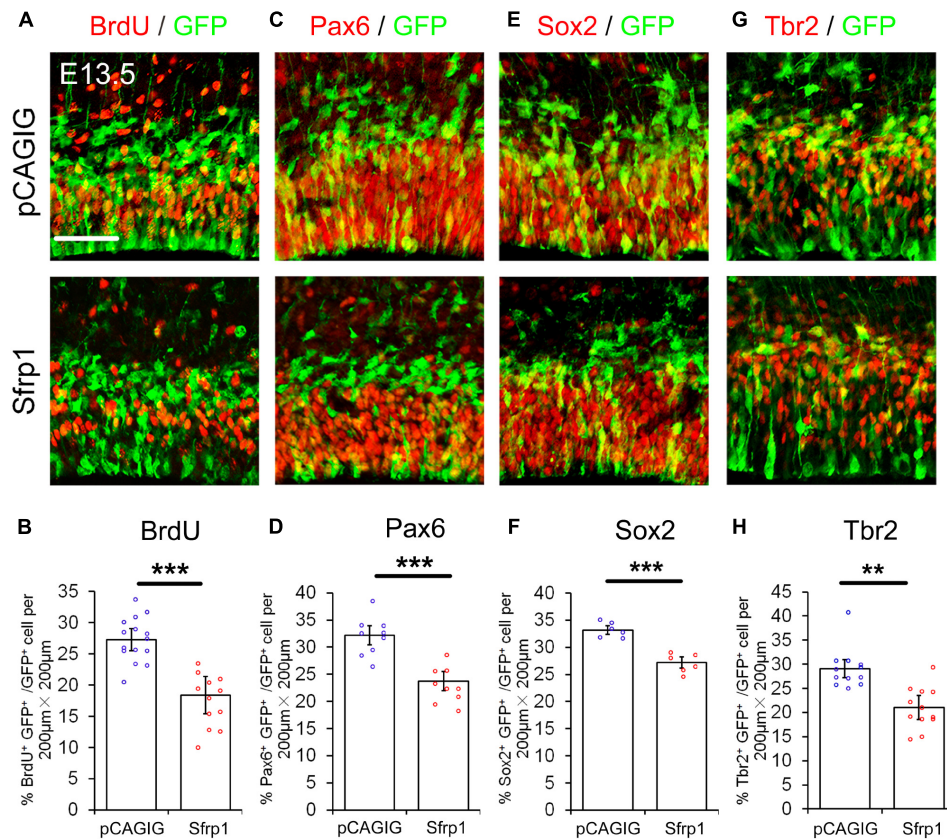


FIGURE 4 | Sfrp1 negatively regulates proliferation of NPs at E13.5. **(A,C,E,G)** Overexpression of *Sfrp1* in E13.5 cortices using *in utero* electroporation, analyzed at E13.5, caused the reduction of BrdU⁺/GFP⁺, Pax6⁺/GFP⁺, Sox2⁺/GFP⁺ and Tbr2⁺/GFP⁺ neural progenitors. **(B,D,F,H)** The proportion of cells labeled with individual progenitor markers and GFP versus cells labeled with GFP was quantified. Values represent mean ± SEM, and each dot represents a data point of the marker⁺ GFP⁺/GFP⁺ % in each section (200 µm × 200 µm). *n* = 3, at least two sections from each brain. ***P* < 0.01; ****P* < 0.001; unpaired Student's *t*-test. Scale bar: 50 µm.

(Supplementary Figure S7). Moreover, increasing *Dkk1* dosage caused a greater decrease in the number of BrdU⁺ and Pax6⁺ cells, suggesting a dosage-dependent antagonistic regulation of *Dkk1* on *Wnt7a* (Supplementary Figure S7).

If *Sfrp1* also has the functions as a *Wnt7a* antagonist, it should have a similar effect to *Dkk1* in NP development. With this in mind, *Wnt7a* and *Sfrp1* were both overexpressed in the cortex using IUE. Similar to *Dkk1*, *Wnt7a-Sfrp1* overexpressed in the VZ caused a reduction of BrdU⁺ and Pax6⁺ cells (Figure 5). Moreover, increasing the dosage of *Sfrp1* had a more profound activity in suppressing *Wnt7a* effect on NP expansion (Figure 5).

Our results suggest that similar to *Dkk1*, *Sfrp1* acts as an antagonist of *Wnt7a* and negatively regulates expansion of NPs.

Sfrp1 Inhibits Wnt7a Activity in TOPflash Luciferase Reporter Assay

Based on the dosage-dependent regulation of *Sfrp1* on *Wnt7a*, we tested whether *Sfrp1* could down-regulate the *Wnt7a* activity. To validate *Sfrp1-Wnt7a* interaction, we used the TOPflash luciferase reporter assay containing the active TCF/LEF binding sites, which is the classical method to identify canonical Wnt/β-catenin

activity (Figure 6A) (Veeman et al., 2003). If the canonical Wnt signaling is activated, the β-catenin will be associated with the TCF/LEF transcription factors to promote the *Firefly luciferase* activity. The mutant TCF/LEF binding site of *FOPflash* was used as the control (Figure 6A).

Wnt1 is a known molecule of the Wnt signaling and is crucial for early development of the CNS (Leal et al., 2011; Cai et al., 2013). As the positive control, we first tested whether *Dkk1* and *Sfrp1* can block *Wnt1* in Neuro2A cells. Compared to the *FOPflash* group, the luciferase activity of *Wnt1* in *Dkk1* overexpression treatment was significantly decreased in the TOPflash group (Figure 6B). Agreed with *Dkk1*, the luciferase activity of *Sfrp1* overexpression showed a similar decrease (Figure 6B).

Next, we tested whether *Sfrp1* can inhibit *Wnt7a* in a similar fashion to how *Wnt1* is negatively regulated in the aforementioned experiment. We found that the luciferase activity of *Wnt7a* was decreased appreciably in both *Sfrp1* and *Dkk1* overexpression treatment, suggesting that *Sfrp1* acts like the known antagonist *Dkk1*, and blocks the *Wnt7a* signal (Figure 6C).

In summary, *Sfrp1* has an attenuating role in Wnt signaling by blocking *Wnt1* and *Wnt7a in vitro*.

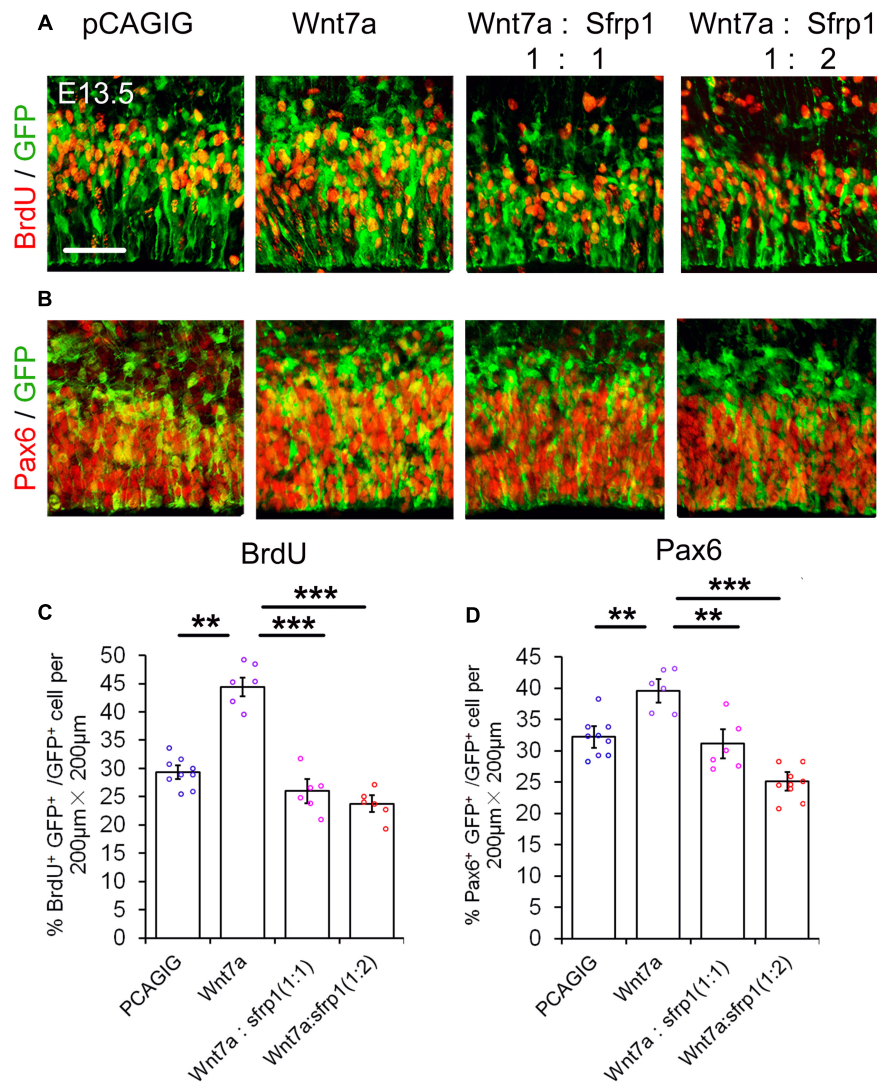


FIGURE 5 | *Sfrp1* suppresses *Wnt7a* activity in neural progenitor proliferation dosage-dependent manner. **(A,B)** Co-expression of *Sfrp1* and *Wnt7a* dampened the effect of *Wnt7a* in expanding neural progenitors at E13.5. **(C,D)** The numbers in BrdU⁺/GFP⁺ and Pax6⁺/GFP⁺ neural progenitors showed a decreasing trend with a proportional increase of *Sfrp1* (*Wnt7a:Sfrp1* = 1:1 vs. *Wnt7a:Sfrp1* = 1:2). Values represent mean ± SEM, and each dot represents a data point of the marker⁺ GFP⁺/GFP⁺ % in each section (200 μm × 200 μm). *n* = 3, at least two sections from each brain. ***P* < 0.01; ****P* < 0.001; unpaired Student's *t*-test. Scale bar = 50 μm.

DISCUSSION

The maintenance of normal cortical formation and size is essential for brain function. The Wnt signaling plays critical roles to regulate cell cycle control, neuronal differentiation and tissue repair (Chenn and Walsh, 2003; Kalani et al., 2008; Piccin and Morshead, 2011; Delaunay et al., 2014). The precise antagonistic regulation of Wnt members by Wnt modulators also controls cortical neurogenesis. Our study shows that *Wnt7a* and *Sfrp1* are co-expressed in cortical NPs and their opposite role is essential for controlling NP expansion and neuronal production.

Among the many signals known to influence the CNS development, the Wnt signal has attracted great attention. Wnt/ β -catenin signaling acts upstream of a complex and dynamic

temporal network to control progenitor fate (Draganova et al., 2015): long-term overexpression of *Wnt3a* leads to cortical dysplasia by inducing early differentiation of IPs into neurons and the heterotopias of these newborn neurons (Munji et al., 2011). Studies have shown the role of *Wnt7a* in axon development and guidance, as well as synapse formation and maintenance (Hall et al., 2000; Cerpa et al., 2008; Ciani et al., 2011, 2015). Investigations of *Wnt7* in the early step of neurogenesis in the cerebral cortex have just begun (Qu et al., 2013; Long et al., 2016). Transcriptome sequencing data from us and others have shown that *Wnt7b*, *Wnt7a*, and *Wnt5a* are the most abundant Wnt factors in the E12.5, E16.5, and E17.5 cortices (Wang et al., 2016; Nguyen et al., 2018). Moreover, we have found that *Wnt7a* is highly expressed in the VZ and *Wnt7b* in the

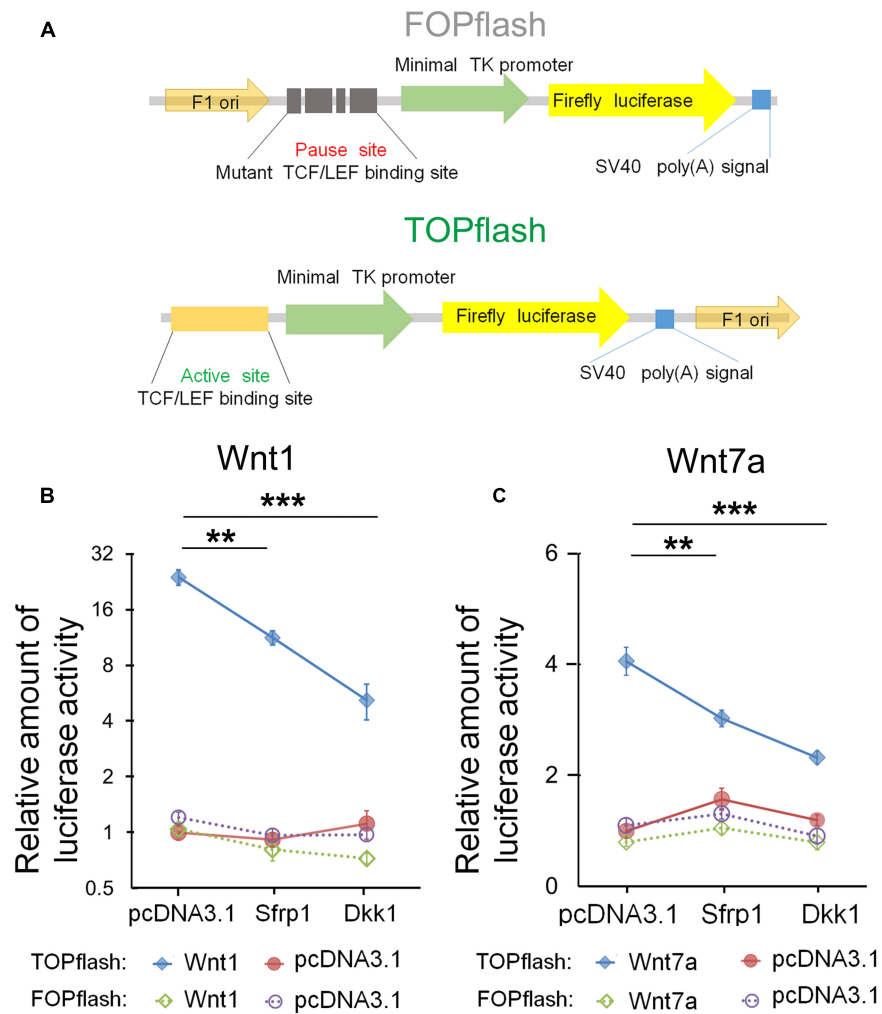


FIGURE 6 | Sfrp1 inhibits *Wnt7a* activity in the *TOPflash* luciferase reporter assay. **(A)** *TOPflash* is a luciferase reporter of β -catenin-mediated transcriptional activation with active TCF/LEF binding sites, which affect the firefly luciferase expression. The control plasmid is *FOPflash*, which contains mutant TCF/LEF binding sites. **(B,C)** After transfection of the *pcDNA3.1-Sfrp1* and *pcDNA3.1-Dkk1*, a statistically significant decrease in luciferase activity of *Wnt1* and *Wnt7a* was observed in comparison with controls. Values represent mean \pm SEM. $n = 3$, $**P < 0.01$; $***P < 0.001$; unpaired Student's *t*-test.

intermediate zone and CP, which is consistent with the RNA-seq results from isolating specific cellular zones and layers in E14.5 and E15.5 cortices (Ayoub et al., 2011; Belgard et al., 2011; Aprea et al., 2013; Liu et al., 2016). How distinct expression patterns of different Wnts are established in developing cortices remains unclear. Differential expression of *Wnt7a* and *Wnt7b* in the cortical layers may determine their different roles in cortical neurogenesis (Stenman et al., 2008; Durak et al., 2016): *Wnt7a* promotes neurogenesis by regulating genes involved in cell cycle control and neuronal differentiation (Qu et al., 2013); the increased *Wnt7b* modulates neuronal differentiation by regulating T-domain transcription factors *Tbr1* and *Tbr2* (Papachristou et al., 2014).

Moreover, we have shown that the deletion of *Wnt7a* expression causes microcephaly by reducing the population of NPs and newborn neurons. These data are consistent with previous reports demonstrating that *Wnt7a* positively regulates

NPs and neurogenesis (Qu et al., 2013; Long et al., 2016; Wang et al., 2016). Recent research has shown that *Wnt7a* regulates the asymmetry of spindles in neuroepithelial cells in the VZ, which is linked to asymmetric cell division (Delaunay et al., 2014). The embryonic ventral midbrain of *Wnt7a* KO mice displays reduced Sox2⁺ progenitors (Fernando et al., 2014). We have also found that Sox2⁺ progenitors are decreased in the cerebral cortex at E13.5. Decreased expansion of cortical NPs is likely a major cause of microcephaly in *Wnt7a* KO mice. Among Wnt molecules, *Wnt7a* is a known regulator in the beta-catenin signal pathway (mmu04310) functioning in different biological processes (Daneman et al., 2009; Ciani et al., 2011; Qu et al., 2013; King et al., 2015). Wnt molecules are associated with Hippo signaling pathway, Integrin signaling and Notch signaling (Qu et al., 2013; Ciani et al., 2015; Wang et al., 2016). These pathways likely cooperate to regulate cortical development.

Sfrps are a family of receptors known to possess a Wnt-binding frizzled CRD, and abnormal expression of *Sfrp1* leads to CNS functional disorders (Esteve et al., 2011, 2018). *Sfrp1* is a key member of the Sfrp family that can bind directly to Wnts via their regions of homology to Fz. In the CNS, *Sfrp1* can block dopamine neuron development, dendritic development and hippocampus formation (Rosso et al., 2005; Miquelajauregui et al., 2007; Kele et al., 2012). In this study, we have found that *Sfrp1* is expressed in the VZ of the mouse embryonic cerebral cortex, which is consistent with the observation of its expression restricted to the proliferative zone in the CNS (Augustine et al., 2001). Similar to the known antagonist *Dkk1*, we have found that overexpression of *Sfrp1* reduces the NP population, and *Sfrp1* significantly decreases the number of NPs in a dosage-dependent manner, suggesting an opposite role of *Sfrp1* in cortical development compare to *Wnt7a* (Adamska et al., 2004; Kim et al., 2008; Osada et al., 2010). In the recent study of *Sfrp1* knockout mice, the authors observed an increase in the number of BrdU⁺/Tbr2⁺ cells in E12.5 *Sfrp1*^{-/-} cortex (Esteve et al., 2018). We think that the reason we did not detect an increase of Tbr2⁺ cells when *Sfrp1* is knocked down, it is likely due to the efficiency of shRNA of *Sfrp1*, compared to the gene knockout. Moreover, recent studies have shown that Sfrps interact with the Wnt signaling, Hedgehog signaling, BMP and Notch signaling (Katoh and Katoh, 2006; Mii and Taira, 2009; Misra and Matise, 2010; Esteve et al., 2011, 2018). It is likely a combined effort of *Sfrp1* with other signals contributes to cortical development.

Sfrps is a physiological Wnt-signaling scavenger that binds directly to Wnts due to their similarity to the receptor Frizzled, thus, it is capable of regulating the availability of Wnt proteins (Finch et al., 1997; Rattner et al., 1997; Baarsma et al., 2013; Cruciat and Niehrs, 2013). The exclusive repression of the Wnt pathway is possible by selective Sfrps in cortical development (Mikels and Nusse, 2006; Lacour et al., 2017). *Sfrp1* and *Sfrp3* are expressed in opposing anterolateral to caudomedial gradients, and regulate normal temporal advancement of neuronal birth and maturation in anterior and lateral cortical regions by selectively modulating Wnts (Kim et al., 2001b). Previous studies have shown that Dkks inhibit the canonical Wnt pathway by internalizing LRP5/6, whereas Sfrps inhibit both the canonical and non-canonical pathways by binding Wnt ligands or Frizzled (Dees et al., 2014; Majchrzak-Celinska et al., 2016). The future

study will be to investigate whether *Sfrp1* directly binds to *Wnt7a* or through other mechanisms in the cortex.

The reciprocal control of *Wnt7a* and *Sfrp1* may be a dosage-dependent compensatory mechanism to maintain normal cortical formation during early development. Our study reveals that an optimal expression level of *Wnt7a* and *Sfrp1* is critical for proper establishment of the NP population. Further work will be dedicated to explore the precise regulation of how different Sfrps mediate canonical Wnt signaling pathway in NP proliferation and differentiation during embryonic cortical development. Our findings suggest that dysregulation of the Wnt signaling can lead to developmental defects similar to human cortical malformation disorders such as microcephaly.

AUTHOR CONTRIBUTIONS

TS: conceived and designed the experiments. NM, SB, TL, and TM: experiment. NM, SB, SH, ZW, GH, and TS: result analysis. NM and TS: wrote the paper. NM and TS: edited paper.

FUNDING

This work was supported by an R01-MH083680 grant from the NIH/NIMH (TS), the National Natural Science Foundation of China (81471152, 31771141, and 81701132), and China Postdoctoral Science Foundation (2017M622053).

ACKNOWLEDGMENTS

We thank members of the Sun Laboratory for their valuable discussions and advice. We thank Dr. Tony Brown for providing reagents, Dr. Julia Kaltschmidt for providing mouse lines, and Drs. Y. Kawase-Koga and Q. Li for technical support.

SUPPLEMENTARY MATERIAL

The Supplementary Material for this article can be found online at: <https://www.frontiersin.org/articles/10.3389/fnmol.2018.00247/full#supplementary-material>

REFERENCES

- Adamska, M., MacDonald, B. T., Sarmast, Z. H., Oliver, E. R., and Meisler, M. H. (2004). *En1* and *Wnt7a* interact with *Dkk1* during limb development in the mouse. *Dev. Biol.* 272, 134–144. doi: 10.1016/j.ydbio.2004.04.026
- Aguirre, A., Rubio, M. E., and Gallo, V. (2010). Notch and EGFR pathway interaction regulates neural stem cell number and self-renewal. *Nature* 467, 323–327. doi: 10.1038/nature09347
- Angers, S., and Moon, R. T. (2009). Proximal events in Wnt signal transduction. *Nat. Rev. Mol. Cell Biol.* 10, 468–477. doi: 10.1038/nrm2717
- Apra, J., Prenninger, S., Dori, M., Ghosh, T., Monasor, L. S., Wessendorf, E., et al. (2013). Transcriptome sequencing during mouse brain development identifies long non-coding RNAs functionally involved in neurogenic commitment. *EMBO J.* 32, 3145–3160. doi: 10.1038/emboj.2013.245
- Ashrafi, S., Lalancette-Hebert, M., Friese, A., Sigrist, M., Arber, S., Shneider, N. A., et al. (2012). *Wnt7A* identifies embryonic gamma-motor neurons and reveals early postnatal dependence of gamma-motor neurons on a muscle spindle-derived signal. *J. Neurosci.* 32, 8725–8731. doi: 10.1523/JNEUROSCI.1160-12.2012
- Augustine, C., Gunnarsen, J., Spirkoska, V., and Tan, S. S. (2001). Place- and time-dependent expression of mouse *sFRP-1* during development of the cerebral neocortex. *Mech. Dev.* 109, 395–397. doi: 10.1016/S0925-4773(01)00533-0
- Ayoub, A. E., Oh, S., Xie, Y., Leng, J., Cotney, J., Dominguez, M. H., et al. (2011). Transcriptional programs in transient embryonic zones of the cerebral cortex defined by high-resolution mRNA sequencing. *Proc. Natl. Acad. Sci. U.S.A.* 108, 14950–14955. doi: 10.1073/pnas.1112213108
- Baarsma, H. A., Konigshoff, M., and Gosens, R. (2013). The WNT signaling pathway from ligand secretion to gene transcription: molecular mechanisms

- and pharmacological targets. *Pharmacol. Ther.* 138, 66–83. doi: 10.1016/j.pharmthera.2013.01.002
- Belgard, T. G., Marques, A. C., Oliver, P. L., Abaan, H. O., Sirey, T. M., Hoerder-Suabedissen, A., et al. (2011). A transcriptomic atlas of mouse neocortical layers. *Neuron* 71, 605–616. doi: 10.1016/j.neuron.2011.06.039
- Bengoa-Vergniory, N., Gorrone-Etxebarria, I., Gonzalez-Salazar, I., and Kypta, R. M. (2014). A switch from canonical to noncanonical Wnt signaling mediates early differentiation of human neural stem cells. *Stem Cells* 32, 3196–3208. doi: 10.1002/stem.1807
- Bengoa-Vergniory, N., and Kypta, R. M. (2015). Canonical and noncanonical Wnt signaling in neural stem/progenitor cells. *Cell. Mol. Life Sci.* 72, 4157–4172. doi: 10.1007/s00018-015-2028-6
- Bovolenta, P., Esteve, P., Ruiz, J. M., Cisneros, E., and Lopez-Rios, J. (2008). Beyond Wnt inhibition: new functions of secreted Frizzled-related proteins in development and disease. *J. Cell Sci.* 121(Pt 6), 737–746. doi: 10.1242/jcs.026096
- Cai, J., Schleidt, S., Pelta-Heller, J., Hutchings, D., Cannarsa, G., and Iacovitti, L. (2013). BMP and TGF-beta pathway mediators are critical upstream regulators of Wnt signaling during midbrain dopamine differentiation in human pluripotent stem cells. *Dev. Biol.* 376, 62–73. doi: 10.1016/j.ydbio.2013.01.012
- Cerpa, W., Godoy, J. A., Alfaro, I., Farias, G. G., Metcalfe, M. J., Fuentealba, R., et al. (2008). *Wnt-7a* modulates the synaptic vesicle cycle and synaptic transmission in hippocampal neurons. *J. Biol. Chem.* 283, 5918–5927. doi: 10.1074/jbc.M705943200
- Chailangkarn, T., Trujillo, C. A., Freitas, B. C., Hrvoj-Mihic, B., Herai, R. H., Yu, D. X., et al. (2016). A human neurodevelopmental model for Williams syndrome. *Nature* 536, 338–343. doi: 10.1038/nature19067
- Chenn, A., and Walsh, C. A. (1999). Perspectives: neurobiology. Cranking it up a notch. *Science* 286, 689–690. doi: 10.1126/science.286.5440.689
- Chenn, A., and Walsh, C. A. (2003). Increased neuronal production, enlarged forebrains and cytoarchitectural distortions in beta-catenin overexpressing transgenic mice. *Cereb. Cortex* 13, 599–606. doi: 10.1093/cercor/13.6.599
- Ciani, L., Boyle, K. A., Dickins, E., Sahores, M., Anane, D., Lopes, D. M., et al. (2011). Wnt7a signaling promotes dendritic spine growth and synaptic strength through Ca²⁺/Calmodulin-dependent protein kinase II. *Proc. Natl. Acad. Sci. U.S.A.* 108, 10732–10737. doi: 10.1073/pnas.1018132108
- Ciani, L., Marzo, A., Boyle, K., Stamatakou, E., Lopes, D. M., Anane, D., et al. (2015). Wnt signalling tunes neurotransmitter release by directly targeting Synaptotagmin-1. *Nat. Commun.* 6:8302. doi: 10.1038/ncomms9302
- Cruciat, C. M., and Niehrs, C. (2013). Secreted and transmembrane wnt inhibitors and activators. *Cold Spring Harb. Perspect. Biol.* 5, a015081. doi: 10.1101/cshperspect.a015081
- Daneman, R., Agalliu, D., Zhou, L., Kuhnert, F., Kuo, C. J., and Barres, B. A. (2009). Wnt/beta-catenin signaling is required for CNS, but not non-CNS, angiogenesis. *Proc. Natl. Acad. Sci. U.S.A.* 106, 641–646. doi: 10.1073/pnas.0805165106
- Dann, C. E., Hsieh, J. C., Rattner, A., Sharma, D., Nathans, J., and Leahy, D. J. (2001). Insights into Wnt binding and signalling from the structures of two Frizzled cysteine-rich domains. *Nature* 412, 86–90. doi: 10.1038/35083601
- Dees, C., Schlottmann, I., Funke, R., Distler, A., Palumbo-Zerr, K., Zerr, P., et al. (2014). The Wnt antagonists DKK1 and SFRP1 are downregulated by promoter hypermethylation in systemic sclerosis. *Ann. Rheum. Dis.* 73, 1232–1239. doi: 10.1136/annrheumdis-2012-203194
- Delaunay, D., Cortay, V., Patti, D., Knoblauch, K., and Dehay, C. (2014). Mitotic spindle asymmetry: a Wnt/PCP-regulated mechanism generating asymmetrical division in cortical precursors. *Cell Rep.* 6, 400–414. doi: 10.1016/j.celrep.2013.12.026
- Draganova, K., Zemke, M., Zurkirchen, L., Valenta, T., Cantu, C., Okoniewski, M., et al. (2015). Wnt/beta-catenin signaling regulates sequential fate decisions of murine cortical precursor cells. *Stem Cells* 33, 170–182. doi: 10.1002/stem.1820
- Durak, O., Gao, F., Kaeser-Woo, Y. J., Rueda, R., Martorell, A. J., Nott, A., et al. (2016). Chd8 mediates cortical neurogenesis via transcriptional regulation of cell cycle and Wnt signaling. *Nat. Neurosci.* 19, 1477–1488. doi: 10.1038/nn.4400
- Esteve, P., Crespo, I., Kaimakis, P., Sandonis, A., and Bovolenta, P. (2018). Sfrp1 modulates cell-signaling events underlying telencephalic patterning, growth and differentiation. *Cereb. Cortex*. doi: 10.1093/cercor/bhy013 [Epub ahead print].
- Esteve, P., Sandonis, A., Cardozo, M., Malapeira, J., Ibanez, C., Crespo, I., et al. (2011). SFRPs act as negative modulators of ADAM10 to regulate retinal neurogenesis. *Nat. Neurosci.* 14, 562–569. doi: 10.1038/nn.2794
- Fernando, C. V., Kele, J., Bye, C. R., Niclis, J. C., Alsanie, W., Blakely, B. D., et al. (2014). Diverse roles for Wnt7a in ventral midbrain neurogenesis and dopaminergic axon morphogenesis. *Stem Cells Dev.* 23, 1991–2003. doi: 10.1089/scd.2014.0166
- Finch, P. W., He, X., Kelley, M. J., Uren, A., Schaudies, R. P., Popescu, N. C., et al. (1997). Purification and molecular cloning of a secreted, Frizzled-related antagonist of Wnt action. *Proc. Natl. Acad. Sci. U.S.A.* 94, 6770–6775. doi: 10.1073/pnas.94.13.6770
- Fortress, A. M., Schram, S. L., Tuscher, J. J., and Frick, K. M. (2013). Canonical Wnt signaling is necessary for object recognition memory consolidation. *J. Neurosci.* 33, 12619–12626. doi: 10.1523/JNEUROSCI.0659-13.2013
- Galli, L. M., Barnes, T., Cheng, T., Acosta, L., Anglade, A., Willert, K., et al. (2006). Differential inhibition of Wnt-3a by Sfrp-1, Sfrp-2, and Sfrp-3. *Dev. Dyn.* 235, 681–690. doi: 10.1002/dvdy.20681
- Garriock, R. J., Chalamalasetty, R. B., Kennedy, M. W., Canizales, L. C., Lewandoski, M., and Yamaguchi, T. P. (2015). Lineage tracing of neuromesodermal progenitors reveals novel Wnt-dependent roles in trunk progenitor cell maintenance and differentiation. *Development* 142, 1628–1638. doi: 10.1242/dev.111922
- Gotz, M., and Huttner, W. B. (2005). The cell biology of neurogenesis. *Nat. Rev. Mol. Cell Biol.* 6, 777–788. doi: 10.1038/nrm1739
- Hall, A. C., Lucas, F. R., and Salinas, P. C. (2000). Axonal remodeling and synaptic differentiation in the cerebellum is regulated by WNT-7a signaling. *Cell* 100, 525–535. doi: 10.1016/S0092-8674(00)80689-3
- Haubensack, W., Attardo, A., Denk, W., and Huttner, W. B. (2004). Neurons arise in the basal neuroepithelium of the early mammalian telencephalon: a major site of neurogenesis. *Proc. Natl. Acad. Sci. U.S.A.* 101, 3196–3201. doi: 10.1073/pnas.0308600100
- Hirabayashi, Y., Itoh, Y., Tabata, H., Nakajima, K., Akiyama, T., Masuyama, N., et al. (2004). The Wnt/beta-catenin pathway directs neuronal differentiation of cortical neural precursor cells. *Development* 131, 2791–2801. doi: 10.1242/dev.01165
- Homem, C. C., Repic, M., and Knoblich, J. A. (2015). Proliferation control in neural stem and progenitor cells. *Nat. Rev. Neurosci.* 16, 647–659. doi: 10.1038/nrn4021
- Ito, H., Morishita, R., Iwamoto, I., and Nagata, K. (2014). Establishment of an in vivo electroporation method into postnatal newborn neurons in the dentate gyrus. *Hippocampus* 24, 1449–1457. doi: 10.1002/hipo.22325
- Joksimovic, M., Yun, B. A., Kittappa, R., Anderegg, A. M., Chang, W. W., Taketo, M. M., et al. (2009). Wnt antagonism of *Shh* facilitates midbrain floor plate neurogenesis. *Nat. Neurosci.* 12, 125–131. doi: 10.1038/nn.2243
- Kalani, M. Y., Cheshier, S. H., Cord, B. J., Bababegy, S. R., Vogel, H., Weissman, I. L., et al. (2008). Wnt-mediated self-renewal of neural stem/progenitor cells. *Proc. Natl. Acad. Sci. U.S.A.* 105, 16970–16975. doi: 10.1073/pnas.0808616105
- Katoh, Y., and Katoh, M. (2006). WNT antagonist, SFRP1, is Hedgehog signaling target. *Int. J. Mol. Med.* 17, 171–175. doi: 10.3892/ijmm.17.1.171
- Kele, J., Andersson, E. R., Villaescusa, J. C., Cajanek, L., Parish, C. L., Bonilla, S., et al. (2012). SFRP1 and SFRP2 dose-dependently regulate midbrain dopamine neuron development in vivo and in embryonic stem cells. *Stem Cells* 30, 865–875. doi: 10.1002/stem.1049
- Kilander, M. B., Dahlstrom, J., and Schulte, G. (2014). Assessment of Frizzled 6 membrane mobility by FRAP supports G protein coupling and reveals WNT-Frizzled selectivity. *Cell. Signal.* 26, 1943–1949. doi: 10.1016/j.cellsig.2014.05.012
- Kim, A. S., Anderson, S. A., Rubenstein, J. L., Lowenstein, D. H., and Pleasure, S. J. (2001a). *Pax-6* regulates expression of *SFRP-2* and *Wnt-7b* in the developing CNS. *J. Neurosci.* 21:RC132.
- Kim, A. S., Lowenstein, D. H., and Pleasure, S. J. (2001b). Wnt receptors and Wnt inhibitors are expressed in gradients in the developing telencephalon. *Mech. Dev.* 103, 167–172.
- Kim, K. A., Wagle, M., Tran, K., Zhan, X., Dixon, M. A., Liu, S., et al. (2008). R-Spondin family members regulate the Wnt pathway by a

- common mechanism. *Mol. Biol. Cell* 19, 2588–2596. doi: 10.1091/mbc.E08-02-0187
- King, M. L., Lindberg, M. E., Stodden, G. R., Okuda, H., Ebers, S. D., Johnson, A., et al. (2015). WNT7A/beta-catenin signaling induces FGF1 and influences sensitivity to niclosamide in ovarian cancer. *Oncogene* 34, 3452–3462. doi: 10.1038/onc.2014.277
- Kuwabara, T., Hsieh, J., Muotri, A., Yeo, G., Warashina, M., Lie, D. C., et al. (2009). Wnt-mediated activation of NeuroD1 and retro-elements during adult neurogenesis. *Nat. Neurosci.* 12, 1097–1105. doi: 10.1038/nn.2360
- Lacour, F., Vezin, E., Bentzinger, C. F., Sincennes, M. C., Giordani, L., Ferry, A., et al. (2017). R-spondin1 controls muscle cell fusion through dual regulation of antagonistic wnt signaling pathways. *Cell Rep.* 18, 2320–2330. doi: 10.1016/j.celrep.2017.02.036
- Lavergne, E., Hendaoui, I., Coulouarn, C., Ribault, C., Leseur, J., Eliat, P. A., et al. (2011). Blocking Wnt signaling by SFRP-like molecules inhibits *in vivo* cell proliferation and tumor growth in cells carrying active beta-catenin. *Oncogene* 30, 423–433. doi: 10.1038/onc.2010.432
- Leal, M. L., Lamas, L., Aoki, M. S., Ugrinowitsch, C., Ramos, M. S., Tricoli, V., et al. (2011). Effect of different resistance-training regimens on the WNT-signaling pathway. *Eur. J. Appl. Physiol.* 111, 2535–2545. doi: 10.1007/s00421-011-1874-7
- Liu, C., Wang, Y., Smallwood, P. M., and Nathans, J. (2008). An essential role for Frizzled5 in neuronal survival in the parafascicular nucleus of the thalamus. *J. Neurosci.* 28, 5641–5653. doi: 10.1523/JNEUROSCI.1056-08.2008
- Liu, J., Wu, X., Zhang, H., Qiu, R., Yoshikawa, K., and Lu, Q. (2016). Prospective separation and transcriptome analyses of cortical projection neurons and interneurons based on lineage tracing by Tbr2 (Eomes)-GFP/Dcx-mRFP reporters. *Dev. Neurobiol.* 76, 587–599. doi: 10.1002/dneu.22332
- Long, K., Moss, L., Laursen, L., Boulter, L., and French-Constant, C. (2016). Integrin signalling regulates the expansion of neuroepithelial progenitors and neurogenesis via Wnt7a and Decorin. *Nat. Commun.* 7:10354. doi: 10.1038/ncomms10354
- Majchrzak-Celinska, A., Slocinska, M., Barciszewska, A. M., Nowak, S., and Baer-Dubowska, W. (2016). Wnt pathway antagonists, *SFRP1*, *SFRP2*, *SOX17*, and *PPP2R2B*, are methylated in gliomas and *SFRP1* methylation predicts shorter survival. *J. Appl. Genet.* 57, 189–197. doi: 10.1007/s13353-015-0312-7
- Menendez, L., Yatskevich, T. A., Antin, P. B., and Dalton, S. (2011). Wnt signaling and a Smad pathway blockade direct the differentiation of human pluripotent stem cells to multipotent neural crest cells. *Proc. Natl. Acad. Sci. U.S.A.* 108, 19240–19245. doi: 10.1073/pnas.1113746108
- Mii, Y., and Taira, M. (2009). Secreted Frizzled-related proteins enhance the diffusion of Wnt ligands and expand their signalling range. *Development* 136, 4083–4088. doi: 10.1242/dev.032524
- Mikels, A. J., and Nusse, R. (2006). Purified Wnt5a protein activates or inhibits beta-catenin-TCF signaling depending on receptor context. *PLoS Biol.* 4:e115. doi: 10.1371/journal.pbio.0040115
- Miquelajauregui, A., Van de Putte, T., Polyakov, A., Nityanandam, A., Boppana, S., Seuntjens, E., et al. (2007). Smad-interacting protein-1 (Zfhx1b) acts upstream of Wnt signaling in the mouse hippocampus and controls its formation. *Proc. Natl. Acad. Sci. U.S.A.* 104, 12919–12924. doi: 10.1073/pnas.0609863104
- Misra, K., and Matisse, M. P. (2010). A critical role for sFRP proteins in maintaining caudal neural tube closure in mice via inhibition of BMP signaling. *Dev. Biol.* 337, 74–83. doi: 10.1016/j.ydbio.2009.10.015
- Molyneaux, B. J., Arlotta, P., Menezes, J. R., and Macklis, J. D. (2007). Neuronal subtype specification in the cerebral cortex. *Nat. Rev. Neurosci.* 8, 427–437. doi: 10.1038/nrn2151
- Morello, F., Prasad, A. A., Rehberg, K., Vieira de Sa, R., Anton-Bolanos, N., Leyva-Diaz, E., et al. (2015). Frizzled3 controls axonal polarity and intermediate target entry during striatal pathway development. *J. Neurosci.* 35, 14205–14219. doi: 10.1523/JNEUROSCI.1840-15.2015
- Munji, R. N., Choe, Y., Li, G., Siegenthaler, J. A., and Pleasure, S. J. (2011). Wnt signaling regulates neuronal differentiation of cortical intermediate progenitors. *J. Neurosci.* 31, 1676–1687. doi: 10.1523/JNEUROSCI.5404-10.2011
- Nathan, E., and Tzahor, E. (2009). sFRPs: a declaration of (Wnt) independence. *Nat. Cell Biol.* 11:13. doi: 10.1038/ncb0109-13
- Nguyen, H., Kerimoglu, C., Pirouz, M., Pham, L., Kiszka, K. A., Sokpor, G., et al. (2018). Epigenetic regulation by BAF complexes limits neural stem cell proliferation by suppressing Wnt signaling in late embryonic development. *Stem Cell Reports* 10, 1734–1750. doi: 10.1016/j.stemcr.2018.04.014
- Osada, M., Jardine, L., Misir, R., Andl, T., Millar, S. E., and Pezzano, M. (2010). DKK1 mediated inhibition of Wnt signaling in postnatal mice leads to loss of TEC progenitors and thymic degeneration. *PLoS One* 5:e9062. doi: 10.1371/journal.pone.0009062
- Papachristou, P., Dyberg, C., Lindqvist, M., Horn, Z., and Ringstedt, T. (2014). Transgenic increase of Wnt7b in neural progenitor cells decreases expression of T-domain transcription factors and impairs neuronal differentiation. *Brain Res.* 1576, 27–34. doi: 10.1016/j.brainres.2014.06.015
- Parr, B. A., and McMahon, A. P. (1995). Dorsalizing signal Wnt-7a required for normal polarity of D-V and A-P axes of mouse limb. *Nature* 374, 350–353. doi: 10.1038/374350a0
- Piccin, D., and Morshead, C. M. (2011). Wnt signaling regulates symmetry of division of neural stem cells in the adult brain and in response to injury. *Stem Cells* 29, 528–538. doi: 10.1002/stem.589
- Prasad, B. C., and Clark, S. G. (2006). Wnt signaling establishes anteroposterior neuronal polarity and requires retromer in *C. elegans*. *Development* 133, 1757–1766. doi: 10.1242/dev.02357
- Qu, Q., Sun, G., Murai, K., Ye, P., Li, W., Asuelime, G., et al. (2013). Wnt7a regulates multiple steps of neurogenesis. *Mol. Cell Biol.* 33, 2551–2559. doi: 10.1128/MCB.00325-13
- Rakic, P. (2007). The radial edifice of cortical architecture: from neuronal silhouettes to genetic engineering. *Brain Res. Rev.* 55, 204–219. doi: 10.1016/j.brainresrev.2007.02.010
- Rakic, P. (2009). Evolution of the neocortex: a perspective from developmental biology. *Nat. Rev. Neurosci.* 10, 724–735. doi: 10.1038/nrn2719
- Rash, B. G., Lim, H. D., Breunig, J. J., and Vaccarino, F. M. (2011). FGF signaling expands embryonic cortical surface area by regulating Notch-dependent neurogenesis. *J. Neurosci.* 31, 15604–15617. doi: 10.1523/JNEUROSCI.4439-11.2011
- Rattner, A., Hsieh, J. C., Smallwood, P. M., Gilbert, D. J., Copeland, N. G., Jenkins, N. A., et al. (1997). A family of secreted proteins contains homology to the cysteine-rich ligand-binding domain of frizzled receptors. *Proc. Natl. Acad. Sci. U.S.A.* 94, 2859–2863. doi: 10.1073/pnas.94.7.2859
- Rosso, S. B., Sussman, D., Wynshaw-Boris, A., and Salinas, P. C. (2005). Wnt signaling through Dishevelled, Rac and JNK regulates dendritic development. *Nat. Neurosci.* 8, 34–42. doi: 10.1038/nn1374
- Rowitch, D. H., S-Jacques, B., Lee, S. M., Flax, J. D., Snyder, E. Y., and McMahon, A. P. (1999). Sonic Hedgehog regulates proliferation and inhibits differentiation of CNS precursor cells. *J. Neurosci.* 19, 8954–8965. doi: 10.1523/JNEUROSCI.19-20-08954.1999
- Saito, T. (2006). *In vivo* electroporation in the embryonic mouse central nervous system. *Nat. Protoc.* 1, 1552–1558. doi: 10.1038/nprot.2006.276
- Saito, T., and Nakatsujii, N. (2001). Efficient gene transfer into the embryonic mouse brain using *in vivo* electroporation. *Dev. Biol.* 240, 237–246. doi: 10.1006/dbio.2001.0439
- Stenman, J. M., Rajagopal, J., Carroll, T. J., Ishibashi, M., McMahon, J., and McMahon, A. P. (2008). Canonical Wnt signaling regulates organ-specific assembly and differentiation of CNS vasculature. *Science* 322, 1247–1250. doi: 10.1126/science.1164594
- Sun, T., and Hevner, R. F. (2014). Growth and folding of the mammalian cerebral cortex: from molecules to malformations. *Nat. Rev. Neurosci.* 15, 217–232. doi: 10.1038/nrn3707
- van Amerongen, R., Mikels, A., and Nusse, R. (2008). Alternative wnt signaling is initiated by distinct receptors. *Sci. Signal.* 1:re9. doi: 10.1126/scisignal.135re9
- Van Raay, T. J., Moore, K. B., Iordanova, I., Steele, M., Jamrich, M., Harris, W. A., et al. (2005). Frizzled 5 signaling governs the neural potential of progenitors in the developing *Xenopus* retina. *Neuron* 46, 23–36. doi: 10.1016/j.neuron.2005.02.023
- Veeman, M. T., Slusarski, D. C., Kaykas, A., Louie, S. H., and Moon, R. T. (2003). Zebrafish prickle, a modulator of noncanonical Wnt/Fz signaling, regulates gastrulation movements. *Curr. Biol.* 13, 680–685. doi: 10.1016/S0960-9822(03)00240-9

- Wang, W., Jossin, Y., Chai, G., Lien, W. H., Tissir, F., and Goffinet, A. M. (2016). Feedback regulation of apical progenitor fate by immature neurons through Wnt7-Celsr3-Fzd3 signalling. *Nat. Commun.* 7:10936. doi: 10.1038/ncomms10936
- Zhao, C., Deng, W., and Gage, F. H. (2008). Mechanisms and functional implications of adult neurogenesis. *Cell* 132, 645–660. doi: 10.1016/j.cell.2008.01.033
- Zhou, Y., and Nathans, J. (2014). Gpr124 controls CNS angiogenesis and blood-brain barrier integrity by promoting ligand-specific canonical wnt signaling. *Dev. Cell* 31, 248–256. doi: 10.1016/j.devcel.2014.08.018

Conflict of Interest Statement: The authors declare that the research was conducted in the absence of any commercial or financial relationships that could be construed as a potential conflict of interest.

Copyright © 2018 Miao, Bian, Lee, Mubarak, Huang, Wen, Hussain and Sun. This is an open-access article distributed under the terms of the Creative Commons Attribution License (CC BY). The use, distribution or reproduction in other forums is permitted, provided the original author(s) and the copyright owner(s) are credited and that the original publication in this journal is cited, in accordance with accepted academic practice. No use, distribution or reproduction is permitted which does not comply with these terms.